RESEARCH ARTICLE | MARCH 04 2019

Electron collisions with $X(CH_3)_4$ molecules (X = C, Si, Ge)

Sylwia Stefanowska-Tur; Paweł Możejko ; Elżbieta Ptasińska-Denga; Czesław Szmytkowski

J. Chem. Phys. 150, 094303 (2019)
https://doi.org/10.1063/1.5086689

The Journal of Chemical Physics ARTICLE scitation.org/journal/jcp

Electron collisions with $X(CH_3)_4$ molecules (X = C, Si, Ge)

Cite as: J. Chem. Phys. 150, 094303 (2019); doi: 10.1063/1.5086689
Submitted: 21 December 2018 • Accepted: 13 February 2019 •
Published Online: 4 March 2019

Sylwia Stefanowska-Tur,[a] Paweł Możejko,[b] Elżbieta Ptasińska-Denga,[c] and Czesław Szmytkowski[d]

AFFILIATIONS

Department of Atomic, Molecular and Optical Physics, Faculty of Applied Physics and Mathematics, Gdańsk University of Technology, ul. Gabriela Narutowicza 11/12, 80-233 Gdańsk, Poland

[a]sylstefa1@student.pg.edu.pl
[b]paw@pg.edu.pl
[c]elzdenga@pg.edu.pl
[d]czsz@mif.pg.gda.pl

ABSTRACT

Absolute *grand*-total cross sections (TCSs) for electron scattering from tetramethylmethane [$C(CH_3)_4$], tetramethylsilane [$Si(CH_3)_4$], and tetramethylgermane [$Ge(CH_3)_4$] molecules have been measured at electron-impact energies extending from around 0.5 to 300 eV in the linear electron-transmission experiment. The measured TCS energy dependences show very pronounced broad enhancement, peaking near 5.5 eV for $Si(CH_3)_4$ and $Ge(CH_3)_4$ molecules and around 6.5 eV for $C(CH_3)_4$. Additional weak structures are also located at higher electron energies. We attributed the TCS features to the resonant processes involved in the electron–molecule scattering. To examine the role of permethylation in the scattering, the measured TCS energy functions for $X(CH_3)_4$ compounds (X = C, Si, Ge) have been compared to the TCS curves for XH_4 molecules. Additionally, the integral elastic cross section (ECS) and ionization cross section (ICS) have been calculated from intermediate to high electron-impact energies using model methods. At energies above 50 eV, the sum of ECS and ICS for the investigated targets is in satisfactory agreement with the respective measured TCS. The computed ECS+ICS values can be used as rough estimation of TCS at energies above 300 eV.

I. INTRODUCTION

Complete information about fundamental collisional processes, including electron-scattering cross-sectional data, reaction rates, and electron transport parameters, is strongly desirable in many scientific areas, extending from ionizing radiation damage to the biomolecules,[1] and plasma physics and chemistry, physics of atmosphere to astrophysics and astrobiology.[2] Reliable electron-scattering measurables for various compounds, especially those containing Si and Ge atoms, are also of great interest in industry[3,4] and current technologies, like plasma-enhanced chemical vapor deposition[5–7] or Focused Electron Beam Induced Deposition (FEBID).[8,9]

Despite the demand for electron scattering data, even for relatively simple though interesting compounds, like $X(CH_3)_4$ (X = C, Si, Ge), absolute values of cross sections are rather scarce. Numerous studies on the interaction of electrons with these molecules exist only for $Si(CH_3)_4$. Electron transmission (ET) experiments of Giordan and Moore[10] and Modelli *et al.*[11] provided energies of electron attachment to the low-energy empty molecular orbital. Inner shell excitation spectra of $Si(CH_3)_4$ were measured by Sodhi *et al.* and Winkler *et al.*[12,13] using the electron energy-loss spectroscopy (EELS). Valence-shell ionization energy spectra were investigated with the (e, 2e) spectroscopy by Daniels *et al.*[14] Kurunczi *et al.*[15] analyzed optical emission induced by electron impact on the $Si(CH_3)_4$ molecules. Vibrational excitation function, electron-energy-loss spectra, and excitation functions of selected electronically excited states were recorded as functions of the incident electron energy, ranging from 0 to 11 eV, by Huber *et al.*[16] Absolute partial and total ionization cross sections

were measured by McGinnis *et al.*[17] and Basner *et al.*[18] from the threshold to 70 eV and 90 eV, respectively. The total ionization cross section of tetramethylsilane has been computed with the binary-encounter-Bethe (BEB) model by Ali *et al.*[19] Further calculations of electron-impact ionization cross sections were carried out by Deutsch *et al.*[20] using the modified additivity rule (MAR) and by Probst *et al.*[21] employing the Deutsch-Märk (DM) formalism. The complex scattering potential–ionization contribution (CSP-*ic*) approach was used by Joshipura *et al.*[22] for calculations of total electron-impact ionization and summed electronic excitation cross sections. The electron drift velocity in $Si(CH_3)_4$ vapor, as a function of the applied uniform electric field, was measured by Faidas *et al.*[23] Yoshida *et al.*[24] measured electron arrival-time spectra and determined the electron drift velocity, the effective ionization, and longitudinal diffusion coefficients. Using these electron transport coefficients and based on the Boltzmann equation solution, Bordage[25] and Hien *et al.*[26] derived a set of electron-collision cross sections over a wide impact-energy range: for the momentum-transfer and electron attachment, for vibrational and electronic excitations, and for total ionization. Recently, a similar set of cross sections was estimated by Kawaguchi *et al.*[27] employing the electron swarm method and the Monte Carlo simulations. The differential, integral, and momentum-transfer cross sections (MTCSs) for elastic electron collisions from $Si(CH_3)_4$ were measured by Sugohara *et al.*[28] at intermediate energies (100–1000 eV) using the crossed-beam scattering geometry. They also computed the total absorption and elastic cross sections employing the independent-atom model (IAM) and the additivity rule (AR) approach.

For $C(CH_3)_4$ and $Ge(CH_3)_4$ molecules, there are only a few reports concerning interaction with electrons. For $C(CH_3)_4$, the decomposition of molecule by electron impact and appearance energies of observed positive ions was reported by Lampe and Field.[29] The momentum transfer cross section was determined by Christophorou and Pittman based on results of their electron swarm experiment[30] and by McCorkle *et al.* from the measured temperature dependence of the electron drift velocity in $C(CH_3)_4$.[31] Also Faidas *et al.*[23] have measured the electron drift velocity in $C(CH_3)_4$ vapor. The derivative electron transmission spectrum was taken by Giordan and Moore.[10] These authors and Modelli *et al.*[11] also reported the electron attachment energy and derivative of the electron transmission current as a function of the incident electron energy for the $Ge(CH_3)_4$ molecule.

Results of most experiments on electron impact by the $X(CH_3)_4$ molecules (X = C, Si, Ge) are limited to a specific range of impact energy and/or report the yield of particular process in arbitrary units only. To the present, no experimental total electron-scattering cross sections (TCSs) for this family of compounds are available in the literature. Thanks to its reliable absolute values, the experimental TCS may serve as a calibration standard or an upper limit reference for normalization of particular cross sections which were determined only in arbitrary units. They can be also applied as one of the ranges of experimental tests of the reliability of theoretical models and computational procedures used for investigations of processes induced by an electron impact.

The aim of the present work was mainly to provide reliable, absolute electron-scattering *grand*–total cross sections (TCSs) for $Si(CH_3)_4$ as well as for $C(CH_3)_4$ and $Ge(CH_3)_4$ molecules. Measurements were carried out for energies ranging from 0.5 to 300 eV using a linear electron transmission technique. Reported TCSs for the family of $X(CH_3)_4$ compounds (X = C, Si, Ge) provide understanding of the role played by the central atom of the target molecule in the electron scattering process and, when compared to TCS data for the XH_4 molecules, insight into the role of methylation. Such findings could also help in predicting scattering quantities for practically important (but usually rather complex) targets, for which relevant data are still lacking due to experimental and/or computational difficulties.

In addition, to extend our TCS results beyond the experimental limit and provide data for elastic and ionization processes at intermediate and high impact energies, we computed integral elastic cross section (ECS) and ionization cross section (ICS) for considered molecules using the additivity rule (AR) approximation and binary-encounter-Bethe (BEB) approach, respectively. Finally, the current ECS and ICS calculations for the $Si(CH_3)_4$ molecule are compared to the existing experimental and/or theoretical data.

II. EXPERIMENTAL

Presented experimental TCS results have been obtained using electrostatic electron spectrometer working in a linear transmission mode. Detailed description of the experimental apparatus and measurement procedure is available elsewhere,[32] and thus only a brief outline is given here. The electrons are generated by the thoriated tungsten filament in the thermionic emission process and formed into the narrow and monoenergetic beam ($\Delta E \leq 0.1$ eV, full width at half-maximum) by the set of electrostatic lens system and 127° cylindrical electrostatic energy selector. The monochromatic electron beam is accelerated to the desired energy E and directed into a scattering chamber, filled with target vapor. The electrons, which leave the reaction cell through the exit orifice, enter into the retarding field analyzer (RFA) where they are energetically discriminated to eliminate those scattered inelastically into the forward direction to be detected by the Faraday cup. The energy scale has been calibrated with respect to the well known resonant oscillatory structure visible around 2.3 eV when the target was mixed with N_2 molecules. The external magnetic field along electron trajectories was reduced to 0.1 μT by the Helmholtz coil system. The electron optics is housed in a high vacuum chamber maintained at the background pressure below 0.1 mPa.

TCS has been determined from the measured quantities using the Bouguer–de Beer–Lambert (BBL) formula,

$$TCS(E) = \frac{k\sqrt{T_m T_t}}{pL} \ln \frac{I_0(E)}{I_t(E)}, \quad (1)$$

where k denotes the Boltzmann constant. $I_0(E)$ and $I_t(E)$ are the intensities of the electron beam, passing the length L through the scattering chamber, taken in the presence and absence of the target molecules, respectively. The target vapor pressure, p, measured by using a capacitance manometer with the head held at constant temperature, T_m = 322 K, was kept within 80–180 mPa range, which ensured single-scattering conditions. The temperature of the scattering cell, T_t, is usually lower than T_m, by 10–20 K. For that reason, recorded values of the target pressure, p, have been corrected taking into account the thermal transpiration effect.[33]

All quantities used for the TCS derivation from the BBL formula [Eq. (1)] are obtained directly in the present experiment, so the normalization procedure is not necessary. The final absolute TCS value at each given electron energy, E, is a weighted mean of results from several measurement series. Statistical uncertainties of presented results were estimated as one standard deviation of a weighted mean from TCSs values obtained in the successive measurement series. For all investigated $X(CH_3)_4$ targets, the statistical uncertainty was well below 1% for energies between 2 and 100 eV, increasing up to 2%–3% below 1 eV and to about 1.5% above 200 eV.

One of the most significant and inevitable systematic errors comes from the fact that the detector assembly does not distinguish electrons scattered elastically into small angles in the forward direction from those not scattered. This *forward-scattering effect* is a characteristic for the electron-transmission technique and leads to the overestimation of measured intensities of the transmitted electron current in the presence of the target. As a result, the measured TCS is underestimated and some changes in the shape of the TCS energy dependence may also occur.[34,35] Estimating the amount by which measured TCS might be lowered due to this effect requires experimental or theoretical information on the angular distribution of the scattered electrons. Only for $Si(CH_3)_4$, differential cross sections (DCSs) on elastic scattering were reported by Sugohara *et al.*,[28] above 100 eV. Based on these data, we have found that at energies beyond 100 eV, the TCS lowering for $Si(CH_3)_4$ may be equal to about 3%–4%. Because no such DCS data concerning $C(CH_3)_4$ and $Ge(CH_3)_4$ molecules have been reported as yet, one can only estimate the TCS lowering for these targets based on respective results for molecular targets of similar structure. Rough estimation shows that due to the forward-scattering, the measured TCSs can be lowered by 4%–5% below 2 eV, about 2%–3% within 20 and 100 eV, and 3%–4% above 150 eV. Note that the TCS data reported in this work are not corrected for the forward-angle-scattering effect.

Another important uncertainty in the electron-transmission experiment is associated with the outflow of target molecules through orifices of the scattering chamber. The effusion of target particles from the scattering cell elongates the effective electron pathway in the target. It also affects the inhomogeneous distribution of the target particle density in the reaction volume, especially close to the orifices. Estimations based on calculations of Nelson and Colgate[36] show that both aforementioned effects may generate the uncertainty of the pL factor in the BBL formula equal of about 2%–3%. In a long-term experiment, a drift in energy occurs, up to 0.1 eV, due to the contamination of the electron optics by target molecules. This effect is the most evident at low electron incident energies, where it can cause a flattening of the structures appearing in the TCS energy dependence. The systematic uncertainty of the measured TCS is estimated as the sum of individual potential systematic errors of all quantities taken in the experiment. It amounts of about 8%–10% below 2 eV, decreasing gradually to 5%–7% within 2 and 6 eV, and to about 5% between 10 and 140 eV, increasing again to 6%–7% at the highest applied energies.

Studied samples [$C(CH_3)_4$ of stated 99% purity from Apollo Scientific and $Si(CH_3)_4$ and $Ge(CH_3)_4$ from Sigma-Aldrich of 99.99+% and 99% purity, respectively] were distilled by freeze-pump-thaw cycles before use.

III. COMPUTATIONAL METHODS

To evaluate the contribution to the scattering process from the elastic and ionization scattering channels and estimate the total cross section for the electron–$X(CH_3)_4$ (X = C, Si, Ge) scattering at energies higher than those available in the present experiment, we have performed simple but reliable numerical calculations. As in our previous studies (see, e.g., Ref. 37 and references therein), the calculated "total" cross section is estimated as the sum of both calculated cross sections, the elastic cross section (ECS) and ionization cross section (ICS). So in the simplified approach, all inelastic scattering channels are neglected, with the exception of ionization. However, we have found that estimated this way, the "total" (elastic+ionization) cross section satisfactorily reproduces the intermediate energy experimental data for variety of molecular targets (Refs. 38–40 and references therein). It is worth noting that ECSs for SiH_4 and GeH_4 molecules, computed with the same approach, are in good agreement with the experimental data.[41]

The ionization cross section has been calculated using the binary-encounter-Bethe (BEB) method.[42,43] Within that model, the total cross section, σ^{Ion}, for electron-impact ionization can be obtained as

$$\sigma^{\mathrm{Ion}} = \sum_{i=1}^{n_{\mathrm{MO}}} \sigma_i^{\mathrm{BEB}}, \tag{2}$$

where n_{MO} is the number of the given molecular orbital. The electron-impact ionization cross section per molecular orbital is given by the following equation:

$$\sigma^{\mathrm{BEB}} = \frac{S}{t+u+1}\left[\frac{\ln t}{2}\left(1-\frac{1}{t^2}\right)+1-\frac{1}{t}-\frac{\ln t}{t+1}\right], \tag{3}$$

where $u = U/B$, $t = T/B$, $S = 4\pi a_0^2 N R^2/B^2$, a_0 = 0.5292 Å, R = 13.61 eV, and T is the energy of impinging electrons. The electron binding energy B, the kinetic energy of the orbital, U, and the orbital occupation number, N, have been calculated for the ground states of the geometrically optimized, within

T_d symmetry, molecules with the Hartree-Fock method using the GAUSSIAN code[44] and the Gaussian 6-311G (2df, 2p) basis set.

Because energies of the highest occupied molecular orbitals (HOMOs) obtained in this way usually differ from experimental ones, we performed also outer valence Green function calculations of correlated electron affinities and ionization potentials[45–48] using the GAUSSIAN code.[44] The resulting values of the ionization thresholds are 11.306, 10.531, and 10.138 eV for $C(CH_3)_4$, $Si(CH_3)_4$, and $Ge(CH_3)_4$, respectively.

The elastic electron scattering with the $X(CH_3)_4$ molecules has been calculated with the additivity rule (AR) approximation (e.g., Refs. 49 and 50) in which the elastic cross section is given by

$$\sigma(E) = \sum_{i=1}^{N} \sigma_i^A(E), \tag{4}$$

where E is an energy of the incident electron; the atomic elastic cross section of the ith atom of the target molecule, $\sigma_i^A(E)$, has been derived according to

$$\sigma^A = \frac{4\pi}{k^2}\left(\sum_{l=0}^{l_{max}}(2l+1)\sin^2\delta_l + \sum_{l=l_{max}+1}^{\infty}(2l+1)\sin^2\delta_l^B\right). \tag{5}$$

To obtain phase shifts, δ_l, partial wave analysis has been employed and the radial Schrödinger equation,

$$\left[\frac{d^2}{dr^2} - \frac{l(l+1)}{r^2} - 2(V_{stat}(r) + V_{polar}(r)) + k^2\right]u_l(r) = 0, \tag{6}$$

has been solved numerically under the boundary conditions

$$u_l(0) = 0, \qquad u_l(r) \overset{r\to\infty}{\longrightarrow} A_l\hat{j}_l(kr) - B_l\hat{n}_l(kr), \tag{7}$$

where $\hat{j}_l(kr)$ and $\hat{n}_l(kr)$ are the Riccati-Bessel and Riccati-Neumann functions, respectively. In the present calculations, the electron-atom interaction has been represented by the static, $V_{stat}(r)$,[51] and polarization, $V_{polar}(r)$,[52] potentials, which are given by following expressions:

$$V_{stat}(r) = -\frac{Z}{r}\sum_{m=1}^{3}\gamma_m \exp(-\beta_m r), \tag{8}$$

where Z is the nuclear charge of the atom and γ_m and β_m are parameters obtained by numerical fitting to the numerical Dirac-Hartree-Fock-Slater screening function;[51]

$$V_{polar}(r) = \begin{cases} \nu(r), & r \le r_c \\ -\alpha/2r^4, & r > r_c \end{cases},$$

where $\nu(r)$ is the free-electron-gas correlation energy,[53] α means the static electric dipole polarizability of atom, and r_c is the first crossing point of the $\nu(r)$ and $-\alpha/2r^4$ curves.[54] In the present calculations, the exact phase shifts have been calculated for l up to $l_{max} = 50$ while those remaining δ_l^B have been included through the Born approximation.

It should be noted that ECSs obtained with the simple AR model can be treated rather as rough approximation. For example, ECSs calculated with the independent atom method (IAM), in which interference terms are accounted for Ref. 55, are distinctly higher than those calculated within AR approximation.

IV. RESULTS AND DISCUSSION

In this section, we report on our absolute *grand*-total cross sections (TCSs) measured for electron collisions from $C(CH_3)_4$, $Si(CH_3)_4$, and $Ge(CH_3)_4$ molecules. Similarities and differences of the measured TCS energy functions are pointed out. Observed TCS features are explained based on the electron-scattering data available for the considered compounds. Next, we compare TCS energy curves for $X(CH_3)_4$ targets (X = C, Si, Ge) with those measured in our laboratory for the family of XH_4 molecules to examine how the replacement of hydrogen atoms with the methyl groups (CH_3) influences the electron-molecule scattering. Finally, we also present our calculated integral elastic cross section (ECS) and ionization cross section (ICS) for electron collision with the $X(CH_3)_4$ molecules, for energies up to 3 keV. The sums, ECS+ICS, are then compared with the measured TCSs.

A. Cross sections for tetramethylmethane [$C(CH_3)_4$], tetramethylsilane [$Si(CH_3)_4$], and tetramethylgermane [$Ge(CH_3)_4$]

Figure 1 displays our absolute electron-scattering total cross sections (TCSs) measured for $X(CH_3)_4$ molecular targets (X = C, Si, Ge) as a function of incident energy in the range 0.4–300 eV for $C(CH_3)_4$, 0.5–300 eV for $Si(CH_3)_4$, and within 0.6–300 eV for the $Ge(CH_3)_4$ molecule. Numerical TCS values for considered targets are collected in Table I. No electron-scattering TCS measurements for the investigated molecules are available in the literature for comparison.

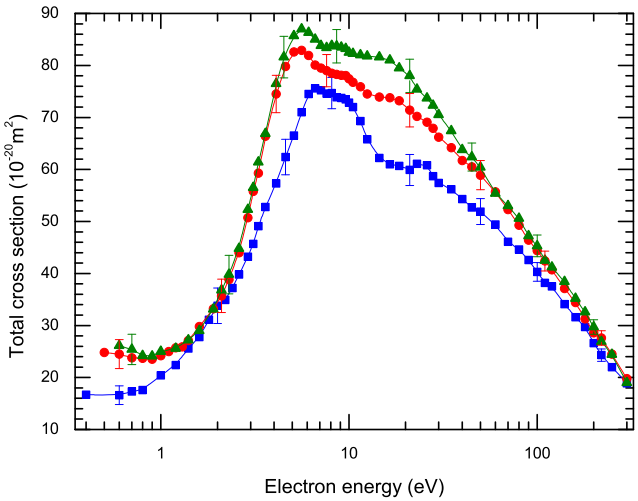

FIG. 1. Present experimental total cross sections for the electron scattering from the $X(CH_3)_4$ molecules (X = C, Si, Ge): full (blue) boxes, $C(CH_3)_4$; full (red) circles, $Si(CH_3)_4$; full (olive) triangles, $Ge(CH_3)_4$; lines added to guide the eyes. Error bars correspond to overall experimental uncertainties.

TABLE I. Absolute experimental electron-scattering total cross sections (TCSs)—at impact energies, E—for the tetramethylmethane [$C(CH_3)_4$], tetramethylsilane [$Si(CH_3)_4$], and tetramethylgermane [$Ge(CH_3)_4$] molecules, in units of 10^{-20} m^2.

	TCS				TCS				TCS		
E (eV)	$C(CH_3)_4$	$Si(CH_3)_4$	$Ge(CH_3)_4$	E (eV)	$C(CH_3)_4$	$Si(CH_3)_4$	$Ge(CH_3)_4$	E (eV)	$C(CH_3)_4$	$Si(CH_3)_4$	$Ge(CH_3)_4$
0.4	16.7			3.3	49.1	59.3	61.4	23	61.1	70.2	75.4
0.5		24.8		3.6	52.8	66.4	66.9	26	60.8	69.1	73.7
0.6	16.6	24.5	26.1	4.1	57.3	74.5	76.5	28	58.7	67.9	72.3
0.7	17.3	23.8	25.4	4.6	62.4	79.8	81.6	30	57.4	66.2	70.5
0.8	17.6	23.7	24.2	5.1	66.5	82.6	85.7	35	56.2	64.2	67.4
0.9		23.5	24.1	5.6	71.0	82.9	87.0	40	54.3	61.7	63.8
1.0	20.4	24.2	25.0	6.1	74.5	81.9	86.3	45	52.7	60.5	62.4
1.1		25.0		6.6	75.6	80.1	85.0	50	51.9	58.9	60.4
1.2	22.4	25.7	25.6	7.1	75.2	79.5	83.8	60	49.4	55.7	55.4
1.3		25.9		7.6	74.6	79.0	83.4	70	46.1	52.3	53.0
1.4	25.6	27.1	27.2	8.1	74.7	78.5	83.8	80	44.6	49.3	50.6
1.6	27.8	29.8	29.0	8.6	73.9	78.3	83.7	90	42.6	46.4	47.2
1.8	31.1			9.1	73.8	78.1	83.5	100	40.3	44.4	45.3
1.9		33.2	33.1	9.6	73.5	78.1	83.2	110	38.2	42.4	42.5
2.0	33.8			10.0	72.8	77.4	82.5	120	37.5	40.7	41.2
2.1		35.7	36.8	10.5	72.0	76.7	82.3	140	34.1	37.1	38.4
2.2	34.9			11.5	69.3	75.9	82.0	160	31.6	34.4	35.2
2.3		38.8	39.8	12.5	65.8	74.5	81.8	180	29.7	31.3	32.6
2.4	37.2			14.5	62.2	73.9	81.6	200	26.6	28.6	29.7
2.6	39.8	44.0	44.8	16.5	61.0	73.8	81.0	220	24.3	27.6	26.9
2.9	43.2	50.7	52.3	18.5	60.7	73.2	79.5	250	22.0	24.5	24.4
3.1	45.7	55.8	56.5	21	59.9	71.4	78.0	300	18.9	19.8	19.0

With respect to the general shape, the TCS curves compared in Fig. 1 are quite similar to one another. The similarity in the shape, and to some degree in the magnitude, is especially evident for $Si(CH_3)_4$ and $Ge(CH_3)_4$ molecules. TCS energy functions depicted in Fig. 1 are dominated by very pronounced broad enhancement peaking within 5–7 eV. Locations of the features visible in the measured TCS energy dependences are listed in Table II. Between 1 and 5.5 eV, TCS curves rise rapidly with energy by more than 50×10^{-20} m^2, although the TCS energy function for $C(CH_3)_4$ is less steep. In the vicinity of 5.6 eV, TCSs for $Si(CH_3)_4$ and $Ge(CH_3)_4$ reach their maximum values of about 83×10^{-20} m^2 and 87×10^{-20} m^2, respectively. The TCS maximum of 76×10^{-20} m^2 for $C(CH_3)_4$ is located at higher energy, near 6.6 eV. Note that these maxima lie below the first electronic excited state of the respective molecule (cf. Table II).

At energies above those of the maximum peaks, on the descending right-hand side of the broad enhancement, each TCS curve shows two additional features: (i) for $Ge(CH_3)_4$, a weak hump centered near 8.6 eV and a shoulder located around 14 eV; (ii) for $Si(CH_3)_4$, a shoulder spanned between 6.5 and 10.5 eV and the second one between 12 and 20 eV; (iii) for $C(CH_3)_4$, between 6.5 and 10.5 eV the TCS slowly decreases to 72×10^{-20} m^2, then rapidly falls to about 60×10^{-20} m^2 near 16 eV, and has a weak hump located around 23 eV. Above 30 eV, the TCS energy functions decline monotonically, and at 300 eV, TCS values fall to about $18–19 \times 10^{-20}$ m^2.

Because the *grand*–TCS represents a sum of scattering information, definitive assignments of broad features visible in the energy dependence of the TCS to particular scattering events are rather uncertain. However, results on the electron–molecule scattering, obtained up to the present, allow us to

TABLE II. Location of the low-energy features, E_{TCS} and E_{ETS}, perceptible in the measured TCS energy dependences and ET spectra, respectively. The energy, E^1_{ex}, of the first excited electronic state. Except otherwise noted, results are from the present experiment.

Molecule	E_{TCS} (eV)	E_{ETS} (eV)	E^1_{ex} (eV)
Tetramethylmethane [$C(CH_3)_4$]	(6.6, 7.5–10, 18–28)	6.1[a]	7.98[b]
Tetramethylsilane [$Si(CH_3)_4$]	(5.6, 8–11, 13–20)	3.9[a]; (3.8, 7.11)[c]; 4.0[d]	7.15[d]
Tetramethylgermane [$Ge(CH_3)_4$]	(5.6, 7–10, 11–18)	3.7[a]; 3.4[c]	

[a]Reference 10.
[b]Reference 66.
[c]Reference 11.
[d]Reference 16.

state that between 3 and 25 eV, some resonant processes contribute to the electron scattering from the considered $X(CH_3)_4$ molecules. In general, the formation of resonant state occurs when the impinging electron of the specific energy is attached to the target molecule yielding a temporary parent negative-ion state.[56] The decay of the resonance may lead to the vibrational excitation of the parent molecule and/or to dissociation into anionic and neutral fragments, manifested as a dramatic increase in respective cross sections within a particular energy range, which—in consequence—can make structures discernible also in the TCS energy function.

To support the statement on the resonant nature of the maximum located between 5 and 6 eV for the $Si(CH_3)_4$ molecule, we turn to results of several low-energy electron-scattering investigations performed for this compound. For $C(CH_3)_4$ and $Ge(CH_3)_4$, the scarcity of experiments and absence of theoretical studies make the interpretation of the TCS features more speculative. At low impact energies, Giordan and Moore[10] measured the derivative electron transmission spectra (ETS) of the tetramethyl compounds of carbon, silicon, and germanium; they also provided the electron attachment energies to these compounds equal of 6.1, 3.9, and 3.7 eV, respectively (see Table II). ETS data of Modelli *et al.*[11] revealed the formation of broad resonances in $Si(CH_3)_4$ and $Ge(CH_3)_4$ molecules, centered around 3.8 and, respectively, at 3.4 eV. The ETS features were assigned to the temporary capture of the incident electron into the lowest unoccupied σ^* molecular orbital located between the central atom and the methyl carbons. Huber *et al.* presented the vibrational excitation function for the $Si(CH_3)_4$ molecule with a spectacular

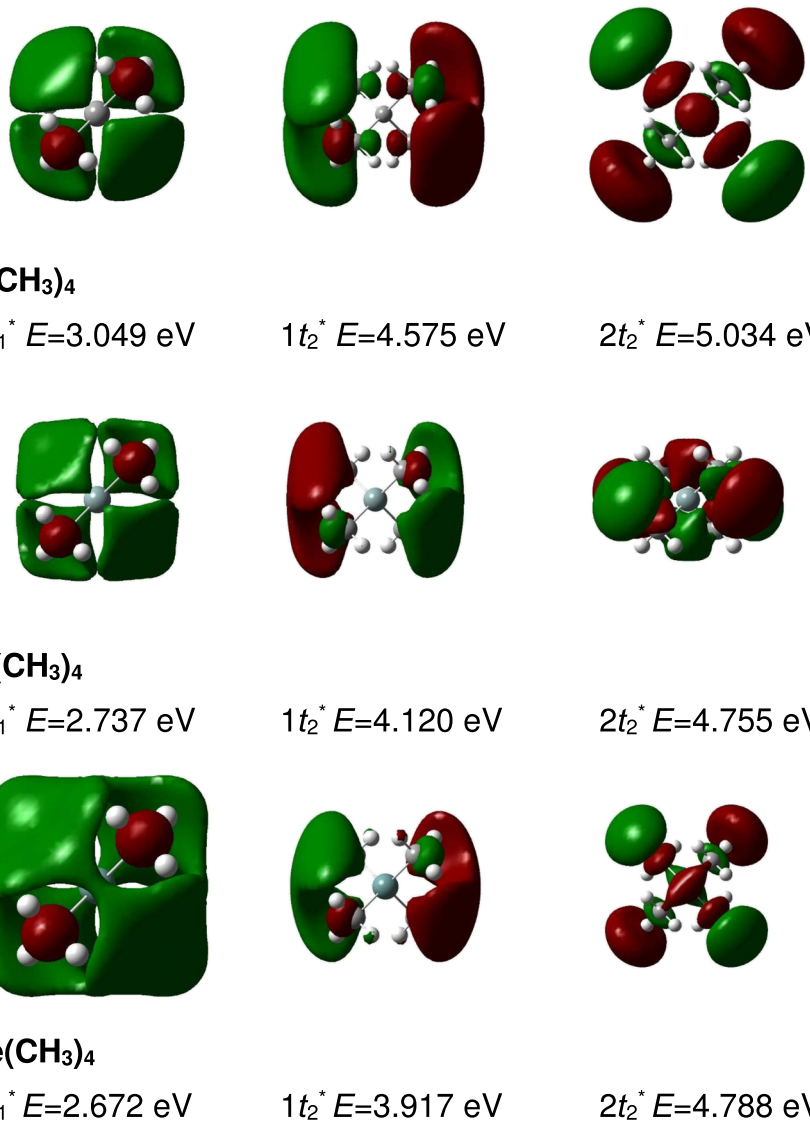

FIG. 2. The first three LUMOs of the $X(CH_3)_4$ molecules (X = C, Si, Ge) calculated with the Gaussian code,[44] using the OVGF method and 6-311** basis set.

enhancement spanned between 2 and 6 eV and the maximum located at 4 eV.[16] This enhancement was also explained by the resonant state formation at around 4 eV. Prompt decay of that resonance via autodetachment of the extra electron leaves the parent molecule in its electronic ground state with the excited C–H vibrations. In the electron energy range between 3 and 7 eV, distinct maxima are also visible in the momentum transfer, vibrational, and dissociative attachment cross sections derived by Bordage,[25] based on electron transport coefficients measured by Yoshida *et al.* in $Si(CH_3)_4$ vapor.[24] The sum of two vibrational cross sections reaches the maximum value of about 10×10^{-20} m^2 near 5 eV[25] (see also in Refs. 26 and 27), which is about 15% of the TCS value at this energy.

Results of ETS experiments[10,11] indicate that also the maximum located between 5 and 6 eV in the TCS curve for $Ge(CH_3)_4$ can be associated with the formation of the negative ion $Ge(CH_3)_4^{*-}$ resonant state in this energy range. Only one report exists[10] for the $C(CH_3)_4$ molecule which confirms the resonant character of electron scattering at around 6.6 eV. The broad feature discerned in the electron transmission spectrum by Giordan and Moore has been explained in terms of the temporarily capture of the incident electron into the σ^* orbital of the $C(CH_3)_4$ molecule. In addition, we have to note that the short-lived σ^* resonances, causing broad bands between 3 and 10 eV in the vibrational excitation functions (related to vibrational modes of the CH_3 target units), were observed also for numerous hydrocarbons (see, e.g., Ref. 57).

It should be also noticed that energies of the lowest unoccupied molecular orbitals (LUMOs) of the studied targets, we calculated with the Gaussian code, lie above 2.5 eV (see Fig. 2). Taking into account the character of these LUMOs, we can speculate that the two lowest t_2^* MOs are involved in the resonances responsible for the maximum observed in the measured TCSs (see Fig. 1).

The structures located on the right from the first peak in TCS energy dependences, presented in Fig. 1, may be associated in part with the opening of inelastic scattering channels, the electronic excitation and ionization. For $Si(CH_3)_4$, experiments of Huber *et al.*[16] suggest that two successive shoulders visible above 6.5 eV in the TCS curve might be related to the electronic excitation of molecule induced by an electron impact: their relative cross section for the excitation of the triplet state peaks near 8.5 eV, close to the center of the TCS shoulder spanned between 6.5 and 10 eV. Moreover, the formation of resonant states above 6.5 eV, associated with the electronic excited states of target molecule, is also possible.

With respect to the TCS magnitudes, Fig. 1 shows that the experimental TCS for $C(CH_3)_4$ is generally lower than those for $Si(CH_3)_4$ and $Ge(CH_3)_4$. Only around 2 eV, the TCS value for all considered molecules is almost the same. On the other hand, the TCS energy curves for $Si(CH_3)_4$ and $Ge(CH_3)_4$ nearly overlap, with the exception of the energy range from 4 to 35 eV, where the TCS for $Ge(CH_3)_4$ is distinctly higher than that for $Si(CH_3)_4$. General similarity in the TCS magnitude for $Si(CH_3)_4$ and $Ge(CH_3)_4$ can be partly associated with the comparable size of both molecules; the pronounced difference only appears at electron impact energies where the role of resonant and/or inelastic processes becomes significant. In the energy range between 4 and 35 eV, the values of TCS compared obey the inequality $TCS[C(CH_3)_4] < TCS[Si(CH_3)_4] < TCS[Ge(CH_3)_4]$. A similar relationship of TCS magnitudes was observed also for the XH_4 compounds (X = C, Si, Ge).[58]

To complement the presented experimental data, it is worth mentioning that in the vicinity of 0.25 eV, the impact energy below the range of the present experiment, the momentum transfer cross section (MTCS) for the $C(CH_3)_4$ molecule exhibits the Ramsauer-Townsend (R-T) minimum.[31] For $Si(CH_3)_4$, the R-T minimum appears in the MTCS energy curve between 0.3 and 0.6 eV.[25–27]

Figure 3 shows our integral elastic cross section (ECS) and ionization cross section (ICS) calculated for $X(CH_3)_4$ molecules (X = C, Si, Ge). Their numerical values are listed in Tables III and IV, respectively. The ECS was obtained in the additive rule approximation[49] with the static+polarization interaction taken into account, while the ICS with the binary-encounter-Bethe approach.[42,43]

In Fig. 3, we also compared our experimental TCSs for considered molecules with sums of respective ECS and ICS; the sum ECS+ICS stands here for the estimation of the overall cross section. In the range of 30–300 eV, where energies of measurements and computations overlap, the theoretical ECS+ICS curves reproduce the TCS measurements rather good, especially with respect to the general shape. It is clear, however, that between 50 and 160 eV, the computed cross

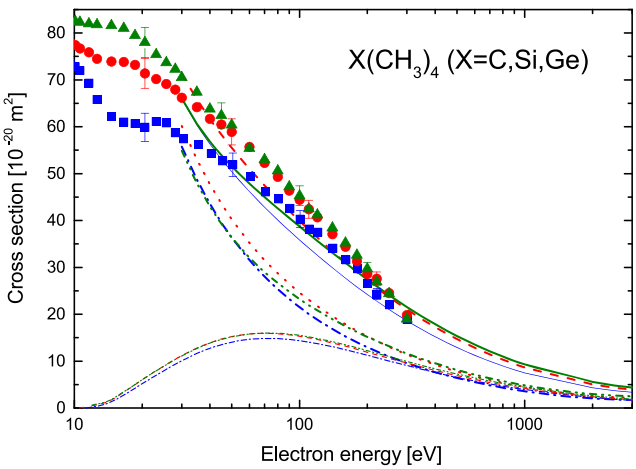

FIG. 3. Comparison of the absolute total cross sections (TCSs) measured in the present experiment for $X(CH_3)_4$ molecules with the cross sections calculated in this work: elastic (ECS), ionization (ICS) and summed (ECS+ICS) cross sections. TCSs, experimental: full (blue) boxes, $C(CH_3)_4$; full (red) circles, $Si(CH_3)_4$; full (olive) triangles, $Ge(CH_3)_4$. ECSs, computed: long dashed-dotted (blue) line, $C(CH_3)_4$; dotted (red) line, $Si(CH_3)_4$; long dash-dot-dot (olive) line, $Ge(CH_3)_4$. ICSs, computed: dashed-dotted (blue) line, $C(CH_3)_4$; dashed (red) line, $Si(CH_3)_4$; dash-dot-dot (olive) line, $Ge(CH_3)_4$. ECS+ICS, computed: fine (blue) line, $C(CH_3)_4$; heavy dashed (red) line, $Si(CH_3)_4$; heavy (olive) line, $Ge(CH_3)_4$. Error bars correspond to overall experimental uncertainties.

TABLE III. Elastic cross sections (ECSs) for electron scattering from $X(CH_3)_4$ molecules (X = C, Si, Ge), in units of 10^{-20} m.[2]

	ECS				ECS		
E (eV)	$C(CH_3)_4$	$Si(CH_3)_4$	$Ge(CH_3)_4$	E (eV)	$C(CH_3)_4$	$Si(CH_3)_4$	$Ge(CH_3)_4$
30	55.8	60.1	54.9	350	8.49	10.2	10.5
35	48.8	53.0	47.9	400	7.64	9.24	9.53
40	43.6	47.7	43.0	450	6.96	8.45	8.76
45	39.6	43.6	39.3	500	6.39	7.79	8.12
50	36.3	40.3	36.4	600	5.50	6.76	7.10
60	31.5	35.2	32.1	700	4.84	5.98	6.33
70	28.0	31.5	29.0	800	4.32	5.38	5.73
80	25.3	28.7	26.6	900	3.91	4.89	5.25
90	23.2	26.5	24.8	1000	3.57	4.49	4.85
100	21.5	24.6	23.2	1100	3.29	4.16	4.52
110	20.0	23.1	21.9	1200	3.06	3.88	4.23
120	18.8	21.7	20.8	1400	2.68	3.43	3.78
140	16.8	19.6	18.9	1600	2.41	3.09	3.44
160	15.3	17.8	17.5	1800	2.20	2.83	3.17
180	14.0	16.4	16.2	2000	2.04	2.63	2.97
200	13.0	15.3	15.2	2200	1.92	2.48	2.81
220	12.1	14.3	14.3	2500	1.80	2.31	2.64
250	11.0	13.1	13.1	3000	1.73	2.19	2.50
300	9.56	11.4	11.6				

sections are systematically lower than the measured TCS values; the differences reach about 13% at 60 eV and 10% in the vicinity of 160 eV. This discrepancy may be partly related to neglecting the excitations of molecules induced in the scattering in our computations. Based on calculations of Joshipura *et al.*[22] we estimated that the contribution of summed

TABLE IV. Electron impact ionization cross section (ICSs) for $X(CH_3)_4$ (X = C, Si, Ge) molecules at energies, *E*, from the ionization threshold up to 3000 eV, in units of 10^{-20} m^2.

	ICS				ICS		
E (eV)	$C(CH_3)_4$	$Si(CH_3)_4$	$Ge(CH_3)_4$	E (eV)	$C(CH_3)_4$	$Si(CH_3)_4$	$Ge(CH_3)_4$
10.138			0.00	85	14.72	15.74	15.86
10.531		0.00		90	14.62	15.62	15.75
11		0.152	0.283	95	14.50	15.47	15.63
11.306	0.00			100	14.36	15.31	15.48
12	0.192	0.493	0.626	110	14.06	14.97	15.17
13	0.482	0.837	0.966	120	13.74	14.61	14.84
14	0.979	1.278	1.378	140	13.08	13.88	14.14
15	1.589	2.028	2.130	160	12.43	13.18	13.47
16	2.303	2.876	2.959	180	11.82	12.52	12.83
17	3.055	3.722	3.788	200	11.26	11.92	12.24
18	3.778	4.533	4.580	225	10.61	11.23	11.57
19	4.493	5.300	5.331	250	10.04	10.62	10.96
20	5.169	6.021	6.037	275	9.517	10.07	10.42
22.5	6.684	7.622	7.606	300	9.048	9.570	9.924
25	7.959	8.955	8.915	350	8.241	8.715	9.071
27.5	9.103	10.16	10.11	400	7.571	8.006	8.360
30	10.08	11.20	11.13	450	7.007	7.410	7.758
35	11.64	12.81	12.72	500	6.525	6.901	7.243
40	12.75	13.93	13.85	600	5.745	6.077	6.405
45	13.53	14.71	14.63	700	5.141	5.440	5.753
50	14.07	15.24	15.19	800	4.658	4.930	5.229
55	14.43	15.59	15.56	900	4.264	4.514	4.799
60	14.66	15.80	15.79	1000	3.934	4.167	4.440
65	14.79	15.91	15.93	1500	2.863	3.035	3.257
70	14.85	15.94	15.99	2000	2.269	2.407	2.594
75	14.84	15.91	15.98	2500	1.888	2.004	2.166
80	14.80	15.84	15.94	3000	1.622	1.722	1.866

electronic excitation cross section, ΣQ_{exc}, to the TCS for $Si(CH_3)_4$ amounts about 15% near 40 eV and 8% around 150 eV. Some lowering of our calculated ECS+ICS with respect to the experimental TCS results is also associated with the neglecting of the multiple and dissociative ionization processes in our ICS calculations; the BEB method provides a lower limit to the experimental "gross" ionization cross section.

In Fig. 4, we compared our computed ECS and ICS for $Si(CH_3)_4$ to experimental and/or theoretical results found in the literature; corresponding results for $C(CH_3)_4$ and $Ge(CH_3)_4$ are unavailable. Concerning the elastic electron scattering from $Si(CH_3)_4$, only measurements of Sugohara *et al.* between 100 and 1000 eV have been reported as yet.[28] Figure 4 reveals that our calculated ECS values lie above the experimental points over the entire energy range, though the differences do not exceed the declared experimental uncertainties. Two experimental total ionization cross-sectional data sets, obtained by McGinnis *et al.*[17] and Basner *et al.*[18] are also depicted in Fig. 4. It is evident that our calculated ICS values are distinctly lower than the measurements of Basner *et al.* while are higher by almost a factor of two than those of McGinnis *et al.* near 70 eV. Other calculated ionization cross sections, those of Probst *et al.*[21] obtained with the Deutch–Märk (DM) formalism and more recent of Joshipura *et al.* with the complex scattering potential–ionization contribution (CSP-*ic*) approach,[22] lie systematically above the present ICS computations. Below 100 eV, our ICS calculation is also lower than results of Deutsch *et al.*,[20] calculated using the modified additivity rule (MAR); in contrast, above 100 eV, the relationship of both calculations is reversed. Note also that the present ICS curve, calculated with the BEB theory, lies slightly above the earlier results of Ali *et al.*[19] obtained with the same theoretical method.

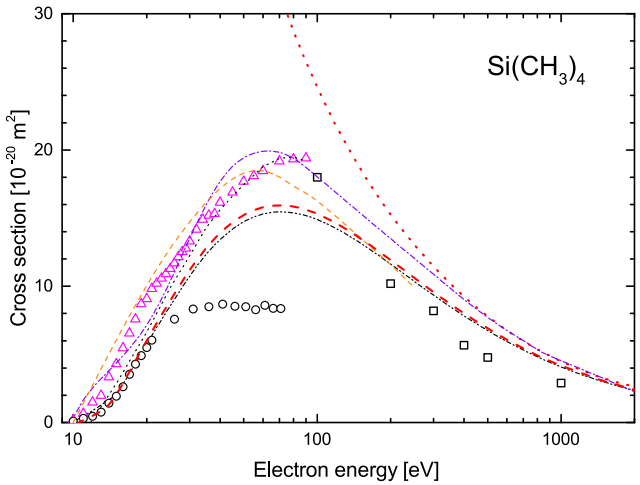

FIG. 4. Comparison of elastic and ionization cross sections for electron collisions with the $Si(CH_3)_4$ molecule, measured and/or calculated (for explanations see the text). Elastic: open (black) boxes, exp., from Ref. 28 and dotted (red) line, computed, present. Ionization, experiments: open (black) circles, from Ref. 17 and open (magenta) triangles, from Ref. 18. Ionization, calculations: heavy dashed (red) line, BEB, present; dash-dot-dot (black) line, BEB, from Ref. 19; dashed (orange) line, MAR, from Ref. 20; dotted (black) line, DM, from Ref. 21; and dashed-dotted (violet) line, CSP-*ic*, from Ref. 22.

B. Comparison of TCSs for electron-scattering from $X(CH_3)_4$ and XH_4 molecules (X = C, Si, Ge): Methylation effect

In this section, we examine how the replacement of four hydrogen atoms in XH_4 molecules (X = C, Si, Ge) with four methyl (CH_3) groups affects the TCS energy dependence for the resulting $X(CH_3)_4$ compounds. For this purpose, in Figs. 5(a)–5(c), we compare our previous experimental TCS energy curves for the family of XH_4 molecules[59–61] to those currently obtained for their permethylated counterparts, $X(CH_3)_4$; experiments for both families of targets were performed with the same experimental system.

Figures 5(a)–5(c) reveal that the substitution of H atoms with the CH_3 groups does not change the shape of TCS energy dependence too much. TCS energy curves for both families of examined compounds have one distinct enhancement with the maximum located below 10 eV. For each of XH_4 molecules, the TCS enhancement is in part related to the formation of the shape resonant state at energy in the vicinity of the TCS maximum (cf. Refs. 62–64 and references therein). Closer examination of Figs. 5(a)–5(c) shows, however, that the TCS maxima in $X(CH_3)_4$ curves are shifted in energy with respect to those for XH_4. For $Si(CH_3)_4$, the TCS maximum shifts toward higher impact energies by 2.7 eV while for $Ge(CH_3)_4$ by 1.8 eV. In effect, around 2 eV–close to the TCS maximum for SiH_4 and GeH_4–the TCS values for these molecules are higher than those for their permethylated derivatives. It is interesting that in contrast to both larger targets, the maximum in the TCS curve for $C(CH_3)_4$ shifts toward lower energies, by about 1.4 eV, with respect to that for CH_4.

A weak effect of methylation is visible also above 10 eV. A barely perceptible feature located near 15 eV in the TCS energy function for CH_4 in the $C(CH_3)_4$ curve becomes more distinct as a small hump centered around 23 eV. A weak shoulder appears also in the vicinity of 15 eV in TCS curves for $Si(CH_3)_4$ and $Ge(CH_3)_4$ molecules. A study on the role of methylation in the ethylene[65] revealed that as a number of methyl groups in a target molecule increase, the TCS structures above 10 eV become more visible and show a steady shift toward higher energies.

It is also evident from Figs. 5(a)–5(c) that the substitution of H atoms with CH_3 groups leads to a distinct increase in the magnitude of TCS for the permethylated derivatives. For instance, around 10 eV, the TCS for $C(CH_3)_4$ is higher than the TCS for CH_4 by a factor of 2.8, while cross sections for the $Si(CH_3)_4$ and $Ge(CH_3)_4$ compounds are higher by a factor of about 1.8 than respective TCSs for SiH_4 and GeH_4. In general, the larger TCS for each permethylated molecule is mainly associated with the increase in its molecular size due to the presence of the methyl units; the gas kinetic cross section for the $C(CH_3)_4$ molecule is more than twice higher than that for CH_4.

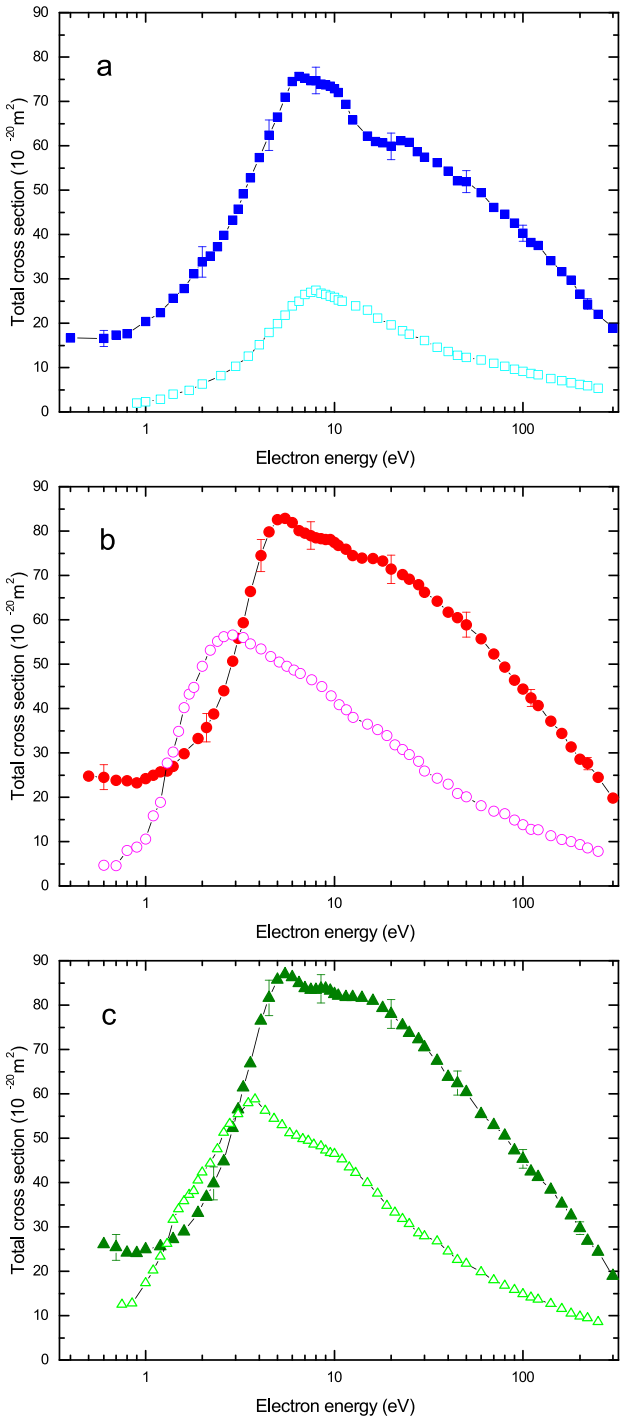

FIG. 5. Comparison of experimental total cross sections for the electron scattering from the $X(CH_3)_4$ and XH_4 molecules (X = C, Si, Ge): (a) full (blue) boxes, $C(CH_3)_4$, present and open (cyan) boxes, CH_4, below 100 eV from Ref. 59, above 100 eV—unpublished results. (b) Full (red) circles, $Si(CH_3)_4$, present and open (magenta) circles, SiH_4, from Ref. 60. (c) Full (olive) triangles, $Ge(CH_3)_4$, present and open (green) triangles, GeH_4, from Ref. 61. Error bars correspond to overall experimental uncertainties.

V. CONCLUSIONS

We have presented experimental absolute total cross sections for electron scattering from $X(CH_3)_4$ molecules (X = C, Si, Ge) measured in this work over the energy range from about 0.5 to 300 eV. Above 1 eV, the TCS energy dependences show a very broad, highly asymmetric enhancement on which some features, located between 4 and 25 eV, are superimposed. These features are attributed to the formation of short-living negative ion states. The replacement of the hydrogen atoms in XH_4 molecules (X = C, Si, Ge) with the CH_3 groups reflects in the cross-sectional energy dependence for permethylated derivatives. For each $X(CH_3)_4$ compound, the main resonant maximum in the TCS curve is shifted in energy with regard to that for the corresponding XH_4 molecule and the amplitudes of TCS features located beyond 10 eV are enlarged. The TCS data reported in this work are not corrected for the forward-scattering effect.

In addition, for $X(CH_3)_4$ molecular targets, the integral elastic cross section (ECS) and ionization cross section (ICS) have been calculated at intermediate and high electron-impact energies in the additivity rule approximation and the binary-encounter-Bethe approach, respectively. For each molecule, the sum of ECS and ICS is in good agreement with the TCS measured above 40 eV. Therefore, the computed ECS+ICS values can be used as a reasonable estimation of TCS at energies above 300 eV. To complete a comprehensive electron scattering data set with cross sections for particular processes, further studies are highly desirable. Differential cross sections for elastic electron scattering would be helpful to estimate corrections of measured TCSs due to the forward scattering effect.

ACKNOWLEDGMENTS

This work has been supported in part by the Polish Ministry of Science and Higher Education (MNiSzW Project 2017-2018). This research was part of the COST Action CM1301 (CELINA). Sylwia Stefanowska kindly acknowledges the support of the Polish Ministry of Science and Higher Education within the Diamond Grant program (Project No. DI2015 018945). Numerical calculations have been performed at the Academic Computer Center (TASK) in Gdańsk.

REFERENCES

[1]L. Sanche, Nature **461**, 358 (2009).
[2]K. Altwegg, H. Balsiger, A. Bar-Nun, J.-J. Bertheller, A. Bieler, P. Bochsler, C. Briois, U. Calmonte, M. R. Combi, H. Cottin, J. De Keyser, F. Dhooghe, B. Fiethe, S. A. Fuselier, S. Gasc, T. I. Gombosi, K. C. Hansen, M. Haessig, A. Jäckel, E. Kopp, A. Korth, L. Le Roy, U. Mall, B. Marty, O. Mousis, T. Owen, H. Réme, M. Rubin, T. Sémon, C.-Y. Tzou, J. H. Waiter, and P. Wurz, Sci. Adv. **2**, e1600285 (2016).
[3]L. G. Christophorou and J. K. Olthoff, *Fundamental Electron Interactions with Plasma Processing Gases* (Kluwer Academic/Plenum Publishers, New York, 2004).
[4]N. J. Mason, J. Phys.: Conf. Ser. **565**, 012001 (2014).
[5]H. Mori and H. Tachikawa, Surf. Coat. Technol. **149**, 224 (2002).
[6]J. Ando, T. Ohmori, A. Murase, N. Takahashi, T. Yamaguchi, and K. Hokkirigawa, Wear **266**, 239 (2009).

[7]A. Soum-Glaude, G. Rambaud, S. E. Grillo, and L. Thomas, Thin Solid Films **519**, 1266 (2010).
[8]A. Perentes and P. Hoffmann, Chem. Vap. Deposition **13**, 176 (2007).
[9]M. Huth, F. Porrati, and O. V. Dobrovolskiy, Microelectron. Eng. **185–186**, 9 (2018).
[10]J. Giordan and J. Moore, J. Am. Chem. Soc. **105**, 6541 (1983).
[11]A. Modelli, D. Jones, L. Fararetto, and G. Distefano, Organometallics **15**, 380 (1996).
[12]R. N. S. Sodhi, S. Daviel, and C. E. Brion, J. Electron Spectrosc. Relat. Phenom. **36**, 395 (1985).
[13]D. C. Winkler, J. H. Moore, and J. A. Tossell, Chem. Phys. Lett. **222**, 1 (1994).
[14]T. A. Daniels, H. Zhu, M. P. Banjavčić, and K. T. Leung, Chem. Phys. **159**, 289 (1992).
[15]P. Kurunczi, A. Koharian, K. Becker, and K. Martus, Contrib. Plasma Phys. **36**, 723 (1996).
[16]V. Huber, K. R. Asmis, A.-C. Sergenton, M. Allan, and S. Grimme, J. Phys. Chem. A **102**, 3524 (1998).
[17]S. McGinnis, K. Riehl, and P. D. Haaland, Chem. Phys. Lett. **232**, 99 (1995).
[18]R. Basner, R. Foest, M. Schmidt, F. Sigenerger, P. Kurunczi, K. Becker, and H. Deutsch, Int. J. Mass Spectrom. Ion Processes **153**, 65 (1996).
[19]M. A. Ali, Y.-K. Kim, W. Hwang, N. M. Weinberger, and M. E. Rudd, J. Chem. Phys. **106**, 9602 (1997).
[20]H. Deutsch, K. Becker, R. Basner, M. Schmidt, and T. D. Märk, J. Phys. Chem. A **102**, 8819 (1998).
[21]M. Probst, H. Deutsch, K. Becker, and T. D. Märk, Int. J. Mass Spectrom. **206**, 13 (2001).
[22]K. N. Joshipura, B. G. Vaishnav, and S. Gangopadhyay, Int. J. Mass Spectrom. **261**, 146 (2007).
[23]H. Faidas, L. G. Christophorou, D. L. McCorkle, and J. G. Carter, Nucl. Instrum. Methods Phys. Res., Sect. A **294**, 575 (1990).
[24]K. Yoshida, S. Mori, Y. Kishimoto, H. Ohuchi, H. Hasegawa, M. Shimozuma, and H. Tagashira, J. Phys. D: Appl. Phys. **38**, 1918 (2005).
[25]M.-C. Bordage, Plasma Sci. Tech. **9**, 756 (2007).
[26]P. X. Hien, D. A. Tuan, and B.-H. Jeon, J. Korean Phys. Soc. **61**, 62 (2012).
[27]S. Kawaguchi, K. Takahashi, K. Satoh, and H. Itoh, Plasma Sources Sci. Technol. **26**, 054001 (2017).
[28]R. T. Sugohara, M.-T. Lee, G. L. C. de Souza, M. G. P. Homem, and I. Iga, Phys. Rev. A **84**, 062709 (2011).
[29]F. W. Lampe and F. H. Field, J. Am. Chem. Soc. **81**, 3238 (1959).
[30]L. G. Christophorou and D. Pittman, J. Phys. B: At. Mol. Phys. **3**, 1252 (1970).
[31]D. L. McCorkle, L. G. Christophorou, D. V. Maxey, and J. G. Carter, J. Phys. B: At. Mol. Phys. **11**, 3067 (1978).
[32]C. Szmytkowski and P. Możejko, Vacuum **63**, 549 (2001).
[33]M. Knudsen, Ann. Phys. **31**, 205 (1910).
[34]J. P. Sullivan, J. Makochekanva, A. Jones, P. Caradonna, D. S. Slaughter, J. Machacek, R. P. McEachran, D. W. Mueller, and S. J. Buckman, J. Phys. B: At., Mol. Opt. Phys. **44**, 035201 (2011).
[35]M. J. Brunger, S. J. Buckman, and K. Ratnavelu, Phys. Chem. Ref. Data **46**, 023102 (2017).
[36]R. N. Nelson and S. O. Colgate, Phys. Rev. A **8**, 3045 (1973).
[37]P. Możejko, C. Szmytkowski, and E. Ptasińska-Denga, Eur. Phys. J. D **66**, 44 (2012).
[38]C. Szmytkowski, A. Domaracka, P. Możejko, E. Ptasińska-Denga, and S. Kwitnewski, J. Phys. B: At., Mol. Opt. Phys. **38**, 745 (2005).
[39]C. Szmytkowski, P. Możejko, S. Kwitnewski, E. Ptasińska-Denga, and A. Domaracka, J. Phys. B: At., Mol. Opt. Phys. **38**, 2945 (2005).
[40]C. Szmytkowski, A. Domaracka, P. Możejko, E. Ptasińska-Denga, Ł. Kłosowski, M. Piotrowicz, and G. Kasperski, Phys. Rev. A **70**, 032707 (2004).
[41]P. Możejko, B. Żywicka-Możejko, and C. Szmytkowski, Nucl. Instrum. Methods Phys. Res., Sect. B **196**, 245 (2002).
[42]Y.-K. Kim and M. E. Rudd, Phys. Rev. A **50**, 3954 (1994).
[43]W. Hwang, Y.-K. Kim, and M. E. Rudd, J. Chem. Phys. **104**, 2956 (1996).
[44]M. J. Frisch *et al*, GAUSSIAN 03, Revision B.05, Gaussian, Inc., Pittsburgh, 2003.
[45]L. S. Cederbaum, J. Phys. B: At. Mol. Phys. **8**, 290 (1975).
[46]W. von Niessen, J. Schirmer, and L. S. Cederbaum, Comput. Phys. Rep. **1**, 57 (1984).
[47]J. V. Ortiz, J. Chem. Phys. **89**, 6348 (1988).
[48]V. G. Zakrzewski and W. von Niessen, J. Comput. Chem. **14**, 13 (1994).
[49]D. Raj, Phys. Lett. A **160**, 571 (1991).
[50]K. N. Joshipura and P. M. Patel, Z. Phys. D: At., Mol. Clusters **29**, 269 (1994).
[51]F. Salvat, J. D. Martinez, R. Mayol, and J. Parellada, Phys. Rev. A **36**, 467 (1996).
[52]N. T. Padial and D. W. Norcross, Phys. Rev. A **29**, 1742 (1984).
[53]J. P. Pedrew and A. Zunger, Phys. Rev. B **23**, 5048 (1981).
[54]X. Zhang, J. Sun, and Y. Liu, J. Phys. B: At., Mol. Opt. Phys. **25**, 1893 (1992).
[55]F. Blanco and G. Garcia, Chem. Phys. Lett. **635**, 321 (2015).
[56]M. Allan, J. Electron Spectrosc. Relat. Phenom. **48**, 219 (1989).
[57]M. Allan and L. Andric, J. Chem. Phys. **105**, 3559 (1996).
[58]C. Szmytkowski, P. Możejko, and G. Kasperski, J. Phys. B: At., Mol. Opt. Phys. **31**, 3917 (1998).
[59]A. Zecca, G. Karwasz, R. S. Brusa, and C. Szmytkowski, J. Phys. B: At., Mol. Opt. Phys. **24**, 2747 (1991).
[60]C. Szmytkowski, P. Możejko, and G. Kasperski, J. Phys. B: At., Mol. Opt. Phys. **30**, 4363 (1997).
[61]P. Możejko, G. Kasperski, and C. Szmytkowski, J. Phys. B: At., Mol. Opt. Phys. **29**, L571 (1996).
[62]M. H. F. Bettega, M. T. do N. Varella, and M. A. P. Lima, Phys. Rev. A **68**, 012706 (2003).
[63]P. Verma, J. Kaur, and B. Antony, Phys. Plasmas **24**, 033501 (2017).
[64]M. Kaur, G. Kaur, A. K. Jain, H. Mohan, P. S. Singh, S. Sharma, and K. L. Baluja, Phys. Rev. A **97**, 052711 (2018).
[65]C. Szmytkowski, S. Stefanowska, M. Zawadzki, E. Ptasińska-Denga, and P. Możejko, J. Chem. Phys. **143**, 064306 (2015).
[66]K. E. Johnson, K. Kim, D. B. Johnston, and S. Lipsky, J. Chem. Phys. **70**, 2189 (1979).